ECERTA

Enabling Certification by Analysis

—

Marie Curie Excellence Team

Start: 01 January 2007
Duration: 48 months

www.cfd4aircraft.com

Report on damping calculations

Prepared by: **Marco Prandina**

Document control data

Deliverable No.:	D **5.2**	Due date:	**01 July 2008**
Version:	**Version 1**	Team Leader:	**Prof. Ken Badcock**
Date delivered:	**08 July 2008**	**Host Organisation : University of Liverpool**	

Project co-funded by the European Commission within the Sixth Framework Programme (2002-2006)		
Dissemination Level		
PU	Public	**x**
PP	Restricted to other programme participants (including the Commission Services)	
RE	Restricted to a group specified by the consortium (including the Commission Services)	
CO	Confidential, only for members of the consortium (including the Commission Services)	

Contents

Abstract **2**

1 Introduction **3**
1.1 Overview of the problem . . . 3
1.2 Adhikari and Woodhouse . . . 3
1.3 Pilkey et al. (Lancaster) . . . 4
1.4 Link's parameterisation . . . 4
1.5 Lee and Kim . . . 4
1.6 Lamarque et al. . . . 5
1.7 Liang and Feeny . . . 5

2 Energy method **6**
2.1 Theory . . . 6
2.2 Example: diagonal viscous damping matrix . . . 7
2.3 Expansion of incomplete measurements . . . 8
2.4 Selection of the most representative degrees of freedom . . . 9

3 Results of numerical simulations **11**
3.1 Viscous damping . . . 11
3.2 Case 1 . . . 12
3.3 Case 2 . . . 13
3.4 Viscous damping and Coulomb friction . . . 14

4 Design of the experiment **15**
4.1 Description of the setup . . . 15
4.2 Description of the setup . . . 15
4.3 Beam design . . . 16
4.4 Viscous dashpot design . . . 17
4.5 Coulomb friction dashpot design . . . 19
4.6 Experiment photographs . . . 19

5 Conclusions **22**

Appendix A **23**

Abstract

This report presents a review of existing damping identification techniques, a new energy-based method derived from one of these techniques and the design of an experiment in order to identify viscous damping and Coulomb friction parameters separately from vibration test of a clamped beam.

Chapter 1

Introduction

1.1 Overview of the problem

Damping is often neglected or over-simplified in dynamic design and modelling of structures. However, there are many cases where an accurate identification of structural damping is very important, especially when the dynamics is dominated by the energy dissipation. If a model is to be used to predict transient responses, transmissibility of exciting forces through the structure, instabilities or decay times, good modelling of damping is necessary. The flutter problem in aircraft wings is an example of a phenomenon dominated by energy dissipation, where accurate damping prediction is important. Unfortunately, damping is still one of the least well-understood aspects of vibration analysis for many reasons. First, there is an absence of a universal mathematical model to represent all damping forces. Secondly, it is not clear which state variables the damping forces will depend on. Finally, damping parameters cannot be measured by the static tests used for stiffness and inertia; dynamic tests, which are normally more effected by noise, are needed. Most of the articles in literature are focused on the identification of viscous damping, i.e. forces dependant on the instantaneous velocities only. This approximation is quite far from reality but in the case of relatively small damping it is reasonable and mathematically convenient for a big range of engineering applications.

1.2 Adhikari and Woodhouse

The paper by Adhikari and Woodhouse [1] proposes a method to identify the viscous damping matrix from the imaginary part of the eigenvalues and eigenvectors obtained from experiments. The method is based on the first order perturbational method and assumes that the damping is small, so eigenvalues and eigenvectors of the damped system will be close to those of the undamped system. The input data for this method are the complex eigenvalues, complex eigenvectors and the mass matrix $\mathbf{M}$ (that can be obtained from an FEM model of the structure) necessary to normalize the eigenvectors to the right scale. This method does not guarantee symmetry in the fitted damping matrix and non-physical results may be obtained, because the original system is reciprocal. The same author also proposed a different model [2] based on the original one (first order perturbational method) that preserves reciprocity of the system forcing the symmetry of the viscous damping matrix $\mathbf{C}$. The results of the numerical simulation of a clamped beam with a dashpot at its free end showed that this method is affected by the

incompleteness of data, especially when the sources of damping are localized in a small number of points and are not distributed. A similar procedure also based on the perturbation method was proposed by Lees [3].

1.3 Pilkey et al. (Lancaster)

Two other methods (one iterative and one direct) to identify the viscous damping matrix were proposed by Pilkey et al. [4] based on the equation derived by Lancaster in his work on the quadratic pencil [5]. The derivation of the equation regarding damping can be found in a more recent paper on the inversion of lambda-matrices and application to the theory of vibrations by Lancaster et al. [6]. The assumptions in this paper are that mass, damping and stiffness matrices are symmetric and the mass matrix is positive definite. The authors also consider that damping is subcritical, so eigenvalues and eigenvectors arise in complex conjugate pairs, but this assumption is not actually necessary and can be ignored simply by reformulating the final equation. Comparing the example used for the method proposed by Adhikari and Woodhouse, this method exhibits better results when dealing with incompleteness of data or noise. One of the drawbacks, for the non-iterative method, is the fact that the stiffness matrix $\mathbf{K}$ has to be known as well as the mass matrix $\mathbf{M}$. These matrices are not usually exactly known in real cases so the identification process can be affected by this uncertainty.

1.4 Link's parameterisation

A common way to represent the damping matrix for large order finite element models is to write it as a linear combination of the mass and stiffness matrices. The so-called proportional damping has no physical meaning but is widely used because it is able to provide real eigenvectors which are more simple to handle compared to complex quantities and reduce the number of parameter to identify from n^2 (n is the number of degrees of freedom of the system) to two. Unfortunately, mode shapes measured by experiments are almost always complex. Link [7] proposes an interesting parameterisation of the viscous damping matrix to be used in model updating of structures. The idea is to represent the full damping matrix of the whole system as a summation of many damping submatrices. These submatrices are proportional to the mass and stiffness matrices of each substructure but the whole matrix is not, so it is able to provide complex mode shapes. Link demonstrates how to use the complex mode shapes in the updating of some selected mass and stiffness uncertain parameters, but also damping parameters, with good experimental results.

1.5 Lee and Kim

Another identification method is proposed by Lee and Kim [8]. This method is able to identify the viscous damping matrix $\mathbf{C}$ from the imaginary part of the inverse of the frequency response function matrix. It is also capable of identifying the hysteretic damping matrix $\mathbf{D}$, the stiffness matrix $\mathbf{K}$ and the mass matrix $\mathbf{M}$ if necessary. The method is based on the fact that the frequency response function matrix (FRM) is the inverse of the dynamic stiffness matrix (DSM)

that contains **C**, **D**, **M** and **K**. Since the FRM is much easier to measure than the DSM, the DSM is obtained by inverting the measured FRM. Then, the **C** and **D** matrices are found by a pseudo-inverse procedure in the frequency domain. The method is validated both numerically and experimentally on a small four degree-of-freedom structure with a dashpot.

1.6 Lamarque et al.

A wavelet-based formula [9] similar to the logarithmic decrement formula used for single degree-of-freedom systems is introduced by Lamarque et al. to estimate damping in multi degree-of-freedom systems from time domain responses. The theory is validated analytically in the context of a general continuous wavelet transform and then numerically by comparison with exact reference solutions in the frame of a superabundant multiresolution analysis. This method is able to identify the damping ratio of dynamic systems and revealed an excellent noise resistance when the signal-to-noise ratio is fairly bad.

1.7 Liang and Feeny

The last method reviewed is proposed by Liang and Feeny [10] for a single degree-of-freedom and then extended by Liang to multiple degree-of-freedom systems [11]. The method is based on the balance of the energy input in the system by external forces and the energy dissipated by damping in the system. The data needed to perform this technique are time histories of the degrees of freedom where the damping is acting; the method is validated with a simulated numerical three degree-of-freedom system and experimentally on an equivalent two loop electrical network consisting of two resistor-inductor-capacitor (RLC) series circuits. One of the advantages of this method is the capability of identifying nonlinear damping sources, one of the drawbacks is the fact that there are two important assumptions: the mass matrix has to be diagonal and the stiffness matrix has to be known.

In the next chapter, the theory of a new method based on energy aimed at overcoming the two approximations of Liang's method is presented. An expansion technique and a subselection method are then used to make it applicable to real problems. Chapter 3 shows the results of numerical simulations to validate the method and chapter 4 illustrates the design of an experimental setup in order to identify viscous damping and Coulomb friction parameters separately from vibration test of a clamped beam. Conclusions and future works are summarized in chapter 5 and teccnical drawings can be found in Appendix A.

Chapter 2

Energy method

2.1 Theory

The equations of motion of a damped multi degree-of-freedom system can be written in the matrix form

$$\mathbf{M}\ddot{\mathbf{x}} + \mathbf{K}\mathbf{x} + \mathbf{D} \cdot \mathbf{f}(\mathbf{x}, \dot{\mathbf{x}}, \ddot{\mathbf{x}}) = \mathbf{a}(t), \tag{2.1}$$

where $\mathbf{M} \in \mathbb{R}^{n \times n}$ is the mass matrix, $\mathbf{K} \in \mathbb{R}^{n \times n}$ is the stiffness matrix, $\mathbf{D} \in \mathbb{R}^{n \times n}$ represents one of the possible damping matrices of coefficients multiplied by $\mathbf{f}(\mathbf{x}, \dot{\mathbf{x}}, \ddot{\mathbf{x}}) \in \mathbb{R}^{n \times 1}$, a function of displacements, velocities or accelerations. $\mathbf{x} \in \mathbb{R}^{n \times 1}$ represents the vector of displacements and $\mathbf{a}(t) \in \mathbb{R}^{n \times 1}$ the excitation input vector. Following a similar method to the one used for the single degree of freedom in [10], eq.(2.1) is premultiplied by $\dot{\mathbf{x}}^T$ and then integrated over time to obtain an energy equation:

$$\int_t^{t+T_1} \dot{\mathbf{x}}^{\mathrm{T}} \mathbf{M}\ddot{\mathbf{x}} \mathrm{d}t + \int_t^{t+T_1} \dot{\mathbf{x}}^{\mathrm{T}} \mathbf{K}\mathbf{x} \mathrm{d}t + \int_t^{t+T_1} \dot{\mathbf{x}}^{\mathrm{T}} \mathbf{D} \cdot \mathbf{f}(\mathbf{x}, \dot{\mathbf{x}}, \ddot{\mathbf{x}}) \mathrm{d}t = \int_t^{t+T_1} \dot{\mathbf{x}}^{\mathrm{T}} \mathbf{a}(t) \mathrm{d}t. \tag{2.2}$$

If the excitation force $\mathbf{a}(t)$ and the response $\mathbf{x}$ are periodic, the integration of conservative components of eq.(2.2) is zero over a full cycle of periodic motion. So if T is the period of the force $\mathbf{a}(t)$, the sum of kinetic and potential energy over this period is zero:

$$\int_t^{t+T} \dot{\mathbf{x}}^{\mathrm{T}} \mathbf{M}\ddot{\mathbf{x}} \mathrm{d}t + \int_t^{t+T} \dot{\mathbf{x}}^{\mathrm{T}} \mathbf{K}\mathbf{x} \mathrm{d}t = 0 \tag{2.3}$$

so eq.(2.2) becomes

$$\int_t^{t+T} \dot{\mathbf{x}}^{\mathrm{T}} \mathbf{D} \cdot \mathbf{f}(\mathbf{x}, \dot{\mathbf{x}}, \ddot{\mathbf{x}}) \mathrm{d}t = \int_t^{t+T} \dot{\mathbf{x}}^{\mathrm{T}} \mathbf{a}(t) \mathrm{d}t. \tag{2.4}$$

Eq.(2.4) represents the balance between the energy dissipated by the damping mechanisms on the left hand side of the equation and the energy input to the system on the right hand side. This equation is the base of the identification method proposed.

In eq.(2.4) the unknowns are represented by the coefficient matrix $\mathbf{D}$. This matrix can be parameterised in several different ways (for example, the parameterisation proposed by Link [7] can be used) and the number of unknowns can vary substantially depending on the parameterisation. By exciting the structure with a certain number of different forces and measuring the responses, in theory it is possible to obtain multiple versions of eq.(2.4) so that the number of equations is bigger than the number of unknown parameters in $\mathbf{D}$ and then proceed to the

identification by solving an inverse problem using least squares techniques. An important aspect of this method is that many of the most common damping models can be expressed in the form $\mathbf{D} \cdot \mathbf{f}(\mathbf{x}, \dot{\mathbf{x}}, \ddot{\mathbf{x}})$ that is necessary to apply the method. Also, there is no need to know the stiffness or mass matrix of the system if the full set of measurements is available. For example, the viscous damping dissipative forces can be expressed in the form

$$\mathbf{d_v} = \mathbf{C} \cdot \dot{\mathbf{x}} \tag{2.5}$$

and the Coulomb friction dissipative forces in the form

$$\mathbf{d_c} = \mathbf{D_c} \cdot \mathrm{sign}(\dot{\mathbf{x}}) \tag{2.6}$$

and so on.

2.2 Example: diagonal viscous damping matrix

The simplest case of diagonal viscous damping matrix is considered to explain how the method works. In this case, the following equations can be substituted into eq.(2.4) to obtain the identification equation:

$$\mathbf{D} = \mathrm{diag}(c_{i,i}) \in \mathbb{R}^{n \times n}, \tag{2.7}$$

$$\mathbf{f}(\mathbf{x}, \dot{\mathbf{x}}, \ddot{\mathbf{x}}) = \dot{\mathbf{x}} \in \mathbb{R}^{n \times 1}, \tag{2.8}$$

where $\mathrm{diag}(c_{i,i})$ is a $n \times n$ matrix with different damping coefficients $c_{i,i}$ in each i^{th} degree of freedom of the diagonal and zero elsewhere. Eq.(2.4) becomes

$$\int_t^{t+T} \dot{\mathbf{x}}^{\mathrm{T}} \mathrm{diag}(c_{i,i}) \dot{\mathbf{x}} \mathrm{d}t = \int_t^{t+T} \dot{\mathbf{x}}^{\mathrm{T}} \mathbf{a}(\mathbf{t}) \mathrm{d}t. \tag{2.9}$$

or

$$c_{1,1} \int_t^{t+T} \dot{x_1}^2 \mathrm{d}t + \ldots + c_{i,i} \int_t^{t+T} \dot{x_i}^2 \mathrm{d}t + \ldots + c_{n,n} \int_t^{t+T} \dot{x_n}^2 \mathrm{d}t = E_a. \tag{2.10}$$

By exciting the structure with m different excitations, multiple version of eq.(2.10) are obtained and then grouped into a single matrix equation on the form:

$$\mathbf{A}\,\mathbf{c} = \mathbf{e} \tag{2.11}$$

where

$$\mathbf{A} = \begin{bmatrix} \int_t^{t+T} \dot{x_1}^2 \mathrm{d}t_{(1)} & \ldots & \int_t^{t+T} \dot{x_n}^2 \mathrm{d}t_{(1)} \\ \ldots & \ldots & \ldots \\ \int_t^{t+T} \dot{x_1}^2 \mathrm{d}t_{(m)} & \ldots & \int_t^{t+T} \dot{x_n}^2 \mathrm{d}t_{(m)} \end{bmatrix}, \in \mathbb{R}^{m \times n} \tag{2.12}$$

$$\mathbf{c} = \begin{bmatrix} c_{1,1} \\ \ldots \\ c_{n,n} \end{bmatrix}, \in \mathbb{R}^{n \times 1} \tag{2.13}$$

$$\mathbf{e} = \begin{bmatrix} E_{a\,(1)} \\ \ldots \\ E_{a\,(m)} \end{bmatrix}. \in \mathbb{R}^{m \times 1} \tag{2.14}$$

If $m > n$, eq.(2.11) can be solved using least squares tecnique to obtain the coefficient of the $\mathbf{D}$ matrix as

$$\mathbf{c} = (\mathbf{A}^{\mathrm{T}}\,\mathbf{A})^{-1}\,\mathbf{A}^{\mathrm{T}}\,\mathbf{e}. \tag{2.15}$$

This simple example shows that if all the measurement of velocities $\dot{x}_1, \ldots, \dot{x}_n$ are available and if it is possible to excite the structure with a number of different excitation m that is bigger than the number of degrees of freedom n, the damping coefficients can be easily estimated. Unfortunately in real structures it is impossible to satisfy these two conditions. Firstly, it is very difficult to measure all the degrees of freedom of a real big structure and secondly, even if it was possible, the number of tests to have $m > n$ could be probably take too much time consuming. For these reasons a method is used to expand the measurements of few degrees of freedom to the whole structure and then another method is used to select the best (or the most representative) degrees of freedom to identify damping.

2.3 Expansion of incomplete measurements

This method uses concepts similar to the ones used by Jalali, Ahmadian and Mottershead in [12]. Consider the full vector of velocities $\dot{\mathbf{x}}_\mathbf{f} \in \mathbb{R}^{n\times 1}$ necessary to calculate the matrix $\mathbf{A}$ of eq.(2.12) and to calculate the vector $\mathbf{e}$ of eq.(2.14). In real experiments it is usually easier and less expensive to measure a set of accelerations in p different degrees of freedom, where $p < n$. Define this set as $\ddot{\mathbf{x}}_\mathbf{m} \in \mathbb{R}^{p\times 1}$. If the damping is small and the system is excited by a single frequency harmonic force close to the k^{th} natural frequency, the acceleration response of the structure may be written in the form

$$\ddot{\mathbf{x}}_\mathbf{f} = \phi_{(k)} \cdot \ddot{q}(t). \tag{2.16}$$

where $\phi_{(k)} \in \mathbb{R}^{n\times 1}$ is the full k^{th} mode shape of the undamped structure (that can be derived from a finite element model) and $\ddot{q}(t)$ is a modal coordinate acceleration. Using this approximation it is possible to estimate $\ddot{q}(t)$ from the experimental results and then substitute into eq.(2.16) to obtain complete data. Consider eq.(2.16) for the incomplete measurements

$$\ddot{\mathbf{x}}_\mathbf{m} = \phi_{m(k)} \cdot \ddot{q}(t). \tag{2.17}$$

where $\phi_{m(k)}$ is the incomplete k^{th} mode shape in the form

$$\phi_{m(k)} = \begin{bmatrix} y_1 \\ \ldots \\ y_p \end{bmatrix} \tag{2.18}$$

for $p < n$ degrees of freedom. Considering the excitation at a single frequency ω, the response of the system will be harmonic too and generally contains higher harmonics due to nonlinearities so the modal coordinate $\ddot{q}(t)$ may be represented using

$$\ddot{q}(t) = \sum_{i=1}^{n} (A_n \sin(n\omega t) + B_n \cos(n\omega t)). \tag{2.19}$$

For simplicity, consider the linear case so eq.(2.19) is reduced to

$$\ddot{q}(t) = A\sin(\omega t) + B\cos(\omega t). \tag{2.20}$$

Substituting eq.(2.20) in eq.(2.17), it is possible to rearrange the equation for each time instant from t_0 to t_{end} in a matrix form so that

$$\begin{bmatrix} y_1\sin(\omega t_0) & y_1\cos(\omega t_0) \\ \cdots & \cdots \\ y_p\sin(\omega t_0) & y_p\cos(\omega t_0) \\ \cdots & \cdots \\ y_1\sin(\omega t_{end}) & y_1\cos(\omega t_{end}) \\ \cdots & \cdots \\ y_p\sin(\omega t_{end}) & y_p\cos(\omega t_{end}) \end{bmatrix} \cdot \begin{bmatrix} A \\ B \end{bmatrix} = \begin{bmatrix} \ddot{x}_1(t_0) \\ \cdots \\ \ddot{x}_p(t_0) \\ \cdots \\ \ddot{x}_1(t_{end}) \\ \cdots \\ \ddot{x}_p(t_{end}) \end{bmatrix}. \tag{2.21}$$

Using a least-squares procedure, A and B can be determinated. Then, the analytical integration of eq.(2.20) can be used to reconstruct the full vector of velocities by using the following two equations

$$\dot{q}(t) = \frac{1}{\omega}(-A\cos(\omega t) + B\sin(\omega t)), \tag{2.22}$$

$$\dot{\mathbf{x}}_\mathbf{f} = \phi_{(k)} \cdot \dot{q}(t). \tag{2.23}$$

2.4 Selection of the most representative degrees of freedom

After performing the expansion, it is now possible to calculate the full matrix $\mathbf{A}$ of the diagonal viscous damping matrix example from the measurements, but there is still the problem of solving an underdetermined system of equations. Considering the matrix $\mathbf{A} \in \mathbb{R}^{m \times n}$ (where n is the number of degrees of freedom of the system and m is the number of tests made), usually $m < n$ so the system has an infinite number of solutions. To find a reasonable solution an angle criterion is used. This angle method was used by Friswell, Mottershead and Ahmadian in [13] for a different application in model updating. It is know from the theory of this method that the vector $\mathbf{e}$ is a linear combination of some columns of the matrix $\mathbf{A}$. These columns corresponds to the degrees of freedom where the damping matrix has non-zero elements. The angle between two vectors a and b can be calculated using the relationship

$$\theta = \frac{a^{\mathrm{T}} b}{\sqrt{a^{\mathrm{T}} a} \cdot \sqrt{b^{\mathrm{T}} b}} \ . \tag{2.24}$$

Among the large number of columns of the matrix $\mathbf{A}$, a certain (s) number of columns with the smallest value of θ is selected. From a vector point of view, these columns are the "more parallel" to the vector $\mathbf{e}$ so they are the ones that will best represent the vector in a 1-dimensional approximation. After selecting these columns, the concept of angle between subspaces is introduced [14]. The angle between two matrices (in this case a matrix containing some columns of $\mathbf{A}$ and a matrix containing the $\mathbf{e}$ vector only) can be calculated with the method now described. Consider the two matrices $\mathbf{F} \in \mathbb{R}^{n \times m}$ and $\mathbf{G} \in \mathbb{R}^{n \times q}$. An orthogonal basis for these subspaces can be obtained by the QR algorithm

$$\mathbf{F} = \mathbf{Q_F R_F} \tag{2.25}$$

$$\mathbf{G} = \mathbf{Q_G R_G} \tag{2.26}$$

where $\mathbf{Q_F}$ and $\mathbf{Q_G}$ are orthogonal matrices of dimension $n \times m$ and $n \times q$ respectively and $\mathbf{R_F}$ and $\mathbf{R_G}$ are upper triangular. If $q < m$ there will be q principal angles between the subspaces, θ_i, which are computed from the singular value decomposition of $\mathbf{Q_F}^{\mathrm{T}}\mathbf{Q_G}$. Thus

$$\cos(\theta_i) = \sigma_i(\mathbf{Q_F}^{\mathrm{T}}\mathbf{Q_G}) \tag{2.27}$$

where $\sigma_i()$ indicates the i^{th} singular value.

Again, it is now possible to select a number s of subsets of two columns of $\mathbf{A}$ that have the smallest angle with $\mathbf{e}$. These subsets were created using combinations of one of the previously selected vectors with the other columns of $\mathbf{A}$. This method can then be applied for bigger subsets of three columns and so on. When the angle between these subsets and $\mathbf{e}$ is sufficiently small, the selection can be stopped and only the selected columns will be used to solve eq.(2.11). In this way, matrix $\mathbf{A}$ becomes of size $s \times m$ and it can be solved with least-squares techniques provided $s < m$. Other constraints can be considered in the method to obtain results with more physical meaning. For example, in the diagonal viscous damping matrix, the values of the damping coefficients must be positive so the energy equation may be solved forcing this additional constraint.

This angle selection corresponds to the spatial location of damping in a real structure. By choosing the columns of $\mathbf{A}$ the method allows the location of the damping sources in the system. The value of damping, instead, depends on solving the energy equation. Engineering knowledge can be used to estimate the possible location of the main damping sources before performing the tests so that the accelerometers can be applied in the choosen degrees of freedom only. In this way there will be no need to expand the measurements and then select the best columns. However, this methodology can be applied to a structure without any usable engineering information.

Chapter 3

Results of numerical simulations

3.1 Viscous damping

Several numerical simulations were performed to test the method. In this section the results obtained from a simple example on a clamped ten-elements contilever beam with four viscous dashpot (Figure 3.1) are shown. The simulated structure is excited with sinusoidal forces at

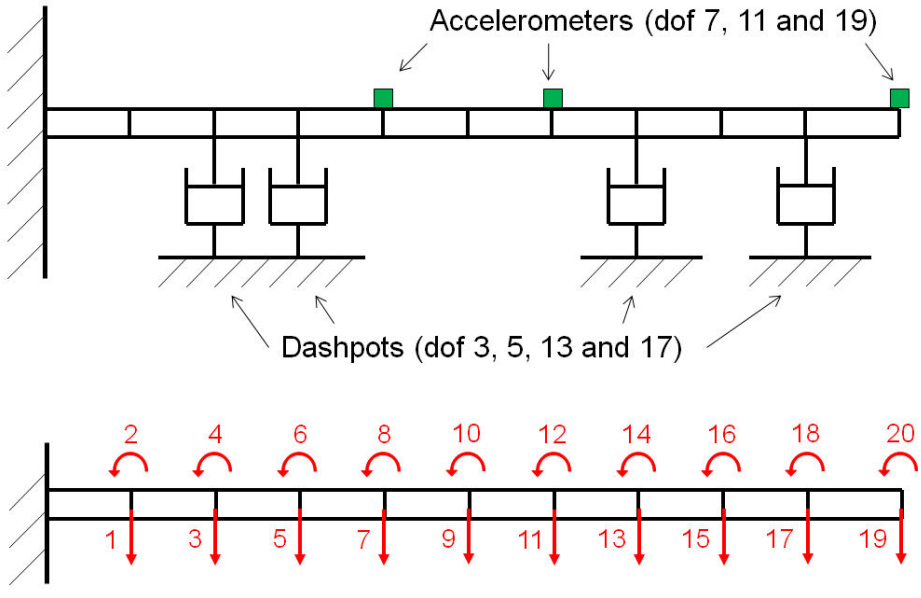

Figure 3.1: Numerical simulation setup

frequencies close to those of the first eight natural modes. From the signal of three accelerometers contaminated with noise, deliberately applied on degrees of freedom without dashpots to demonstrate the robustness of the method even when there are no information about the location of damping, the full vector of velocities is derived and the location and identification of damping is obtained by the methods just explained.

In this example the viscous damping matrix size is 20×20 with only four values different from zero on the diagonal corresponding to the degrees of freedom of the dashpots. Without knowing anything about the structure, the actual number of unknowns of the identification problem is 400 (the number of coefficients in the C matrix). Since the dashpots are connected to the ground

and there are no sources of damping between two elements, the number of unknowns can be reduced to 20 (the diagonal). The matrix **A** described in the previous section will be 8×20 in this example, using 8 different excitations to try to identify the diagonal of the **C** matrix. Two cases are presented with two different sets of values for the damping coefficients of the four dashpots: in case 1 the values are all equal whereas in case 2 the values are different.

Case	**DOF of dashpots**				**Value of damping coefficients [N·s/m]**			
1	3	5	13	17	0.1	0.1	0.1	0.1
2	3	5	13	17	0.01	0.5	0.1	1

Table 3.1: Dashpot configurations in case 1 and case 2

The two examples in Table 3.1 look very similar but they are useful to show what happens when the location of damping based on the angle selection does not work correctly (Case 1) or it does (Case 2).

3.2 Case 1

The identified damping coefficients for case 1 are summarized in Table 3.2. The 'number of dashpots' represents the number of columns of matrix **A** selected to identify the damping. 'Angle' is the angle between the selected columns and the vector **e** of input energies.

Number of dashpots	**DOF of dashpots**				**Value of damping coefficients [N·s/m]**				**Angle**
1	-	-	-	19	-	-	-	0.107	6.505
2	-	-	13	19	-	-	0.151	0.059	0.404
3	-	5	15	17	-	0.212	0.127	0.055	0.124
4	3	5	13	17	0.1	0.1	0.1	0.1	0.000

Table 3.2: Results for case 1

In this case, the location of the dashpots is not always correct. However, considering for example the case with three dashpots, the degree of freedom 15 is close to the correct one 13 and the value of damping coefficients are not so different considering the different locations. In particular, the damping coefficient of the dashpot in 5 is almost the sum of the dashpots in 3 and 5 of the original system. Considering the fact that we are using three dashpots to represent a four-dashpot system and it was assumed absolutely no knowledge about the location and values of the dashpots, this is still a reasonably good result. Even the 'wrong' solutions still hold some useful information. Moreover the identified systems can be considered as an energy equivalent approximation of the original system. This can be noticed by comparing the damping ratio ζ of the first 10 modes of the identified system with the original system (Table 3.3).

Obviously, the agreement between the two systems increases with the number of columns selected. It must be said that an error of $10 \div 20\%$ in the identified damping ratio is acceptable

Mode	ζ Original	ζ 1 dashp.	Err %	ζ 2 dashp.	Err %	ζ 3 dashp.	Err %
1	1.41E-02	1.35E-02	4.09%	1.41E-02	0.14%	1.41E-02	0.13%
2	1.50E-03	2.16E-03	44.15%	1.50E-03	0.07%	1.50E-03	0.22%
3	1.02E-03	7.71E-04	24.74%	8.95E-04	12.60%	1.04E-03	1.22%
4	3.38E-04	3.94E-04	16.66%	3.05E-04	9.68%	3.41E-04	0.95%
5	1.38E-04	2.39E-04	73.13%	1.49E-04	7.97%	1.34E-04	2.90%
6	1.90E-04	1.61E-04	14.82%	1.93E-04	1.99%	1.81E-04	4.51%
7	1.14E-04	1.17E-04	2.68%	1.18E-04	4.23%	1.01E-04	11.37%
8	5.75E-05	8.85E-05	53.99%	4.88E-05	15.07%	4.84E-05	15.81%
9	1.06E-04	6.84E-05	35.49%	7.30E-05	31.11%	1.05E-04	0.51%
10	8.51E-05	4.43E-05	47.96%	6.14E-05	27.87%	8.73E-05	2.62%

Table 3.3: Damping ratios for case 1

and it is also important to notice that the 9^{th} and 10^{th} damping ratio are still reasonably close to the exact solution even if the data used to identify the damping has been derived from excitations close to the first 8 natural frequencies. Another possibility to increase the number of equations for the energy method is not only by exciting the structure at different frequencies but also at different amplitudes. This is useless in this linear example but can be very useful especially in the identification of nonlinearities.

3.3 Case 2

The results obtained for case 2 are qualitatively better than case 1. Especially the location of the main sources of damping is always correct (Table 3.4).

Number of dashpots	DOF of dashpots				Value of damping coefficients [N·s/m]				Angle
1	-	-	-	17	-	-	-	1.084	12.557
2	-	5	-	17	-	0.581	-	1.042	1.029
3	-	5	13	17	-	0.506	0.124	0.989	0.263
4	3	5	13	17	0.01	0.5	0.1	1	0.001

Table 3.4: Results for case 2

An important point that can be noticed from the value of the identified coefficients in Table 3.4 is that not only the right locations are identified but also the sources of damping are selected from the biggest to the smallest when increasing the number of dashpots to identify. This is an interesting result because if the number of columns selected is smaller than the real number of dashpots of the structure, the method can still identify the biggest and then can be considered the most reasonable approximation at that level.

3.4 Viscous damping and Coulomb friction

The method is also tested on a system containing nonlinear damping, i.e. some Coulomb friction devices attached to the previous example structure. In particular, the structure is the ten-elements cantilever beam with three viscous dashpots (in degrees of freedom 3, 13 and 17 with values respectively 0.2 N·s/m, 0.5 N·s/m, 0.15 N·s/m) and three Coulomb friction devices (in degrees of freedom 7, 15 and 19 with values respectively 3.2 N, 5.1 N, 1 N).

	Viscous damping			**Coulomb Friction**		
DOF	3	13	17	7	15	19
Value	0.2 Ns/m	0.5 Ns/m	0.15 Ns/m	3.2 N	5.1 N	1 N

Table 3.5: Dashpot configurations in mixed viscous damping and Coulomb friction case

The method works exactly in the same way of the diagonal viscous damping example, with two small differencies: firstly, the expansion procedure has to consider eq.(2.19) when dealing with nonlinearities and secondly the matrix $\mathbf{A}$ is now 8×40 because the number of unknowns is doubled due to adding the Coulomb friction coefficients identification to the problem. Matrix $\mathbf{A}$ now contains 20 columns of integrals of x_i^2 and 20 columns of integrals of $x_i \cdot \text{sign}(x_i)$.

Number of Dashpots							
1	**DOF**	-	-	-	-	13(C)	-
	Value	-	-	-	-	35.3 N	-
2	**DOF**	-	-	-	13(C)	15(C)*	-
	Value	-	-	-	29.7 N	4.6 N	-
3	**DOF**	-	13(V)*	-	-	15(C)*	19(C)*
	Value	-	0.45 Ns/m	-	-	8.4 N	6.2 N
4	**DOF**	3(V)*	11(V)	13(V)*	17(V)*	-	-
	Value	0.36 Ns/m	0.06 Ns/m	0.51 Ns/m	0.25 Ns/m	-	-
5	**DOF**	3(V)*	7(V)	13(V)*	17(V)*	15(C)*	-
	Value	0.28 Ns/m	0.08 Ns/m	0.52 Ns/m	0.20 Ns/m	3.4 N	-
6	**DOF**	3(V)*	13(V)*	17(V)*	7(C)*	15(C)*	19(C)*
	Value	0.20 Ns/m	0.5 Ns/m	0.15 Ns/m	3.18 N	5.08 N	1 N

Table 3.6: Results of mixed viscous damping and Coulomb friction case: (C) indicates that the degree of freedom identified is related to Coulomb friction, (V) indicates Viscous damping, * indicates correctly identified location.

At present, the angle selection of the columns of the matrix $\mathbf{A}$ when adding nonlinearities seems to be less efficient than in the case with viscous damping only. For this reason, the equivalent identification is not always representative of the spatial location of dashpots. This problem affects the location only whereas the value of damping coefficients can still be well identified if the locations are known. The next step of the research will be to improve especially the location of the damping sources and to extend the method to include material damping.

Chapter 4

Design of the experiment

4.1 Description of the setup

This section presents a description of the design of an experimental setup in order to identify viscous damping and Coulomb friction parameters separately from vibration test of a clamped beam. The two different sources of energy dissipation are respectively obtained by an eddy current magnetic dashpot acting on one side of the beam and two contact friction surfaces on the opposite side. The aim of the experiment is to demonstrate the possibility of locating and evaluate the different types of damping in different spatial configurations.

4.2 Description of the setup

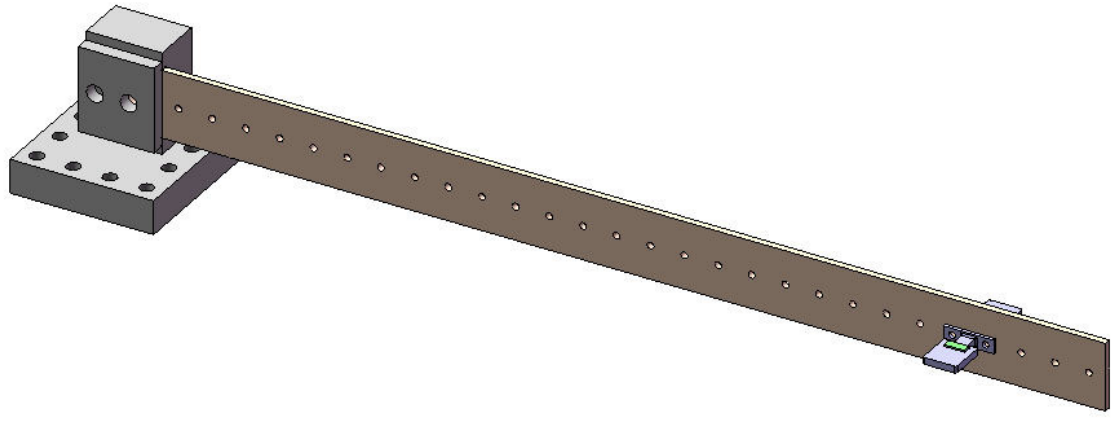

Figure 4.1: Sketch of the beam with wings attached

The experimental setup is composed of:

- An aluminium beam (660×40×4 mm) with 19 equidistant holes in order to obtain 18 different locations for the damping devices through the length of the beam. The beam is clamped at one side and free to move at the other (Figure 4.1).
- 2 aluminium wings (25×20×6 mm) to be connected to the beam by screws.
- 2 NdFeB magnets (10×15×30 mm) with residual magnetic induction equal to 1.2 Tesla to produce the magnetic field for the eddy current dashpot acting on one of the two wings.

- Several different material films to be attached to the other wing to obtain different value for the Coulomb friction

- A small calliper to apply the normal force to the friction device.

4.3 Beam design

The dimensions and material of the beam are designed so that the natural frequencies of the first 10 modes are well separated from each other to minimise the effect of each mode on those closest to it. Starting from a beam with a rectangular 40×4 mm section, an eigenvalue analysis based on a finite element model provides an optimal length of about 560 mm (Figure 4.2). The beam is made of aluminium to avoid magnetic interactions with the magnets, even if they are sufficiently far from the beam itself.

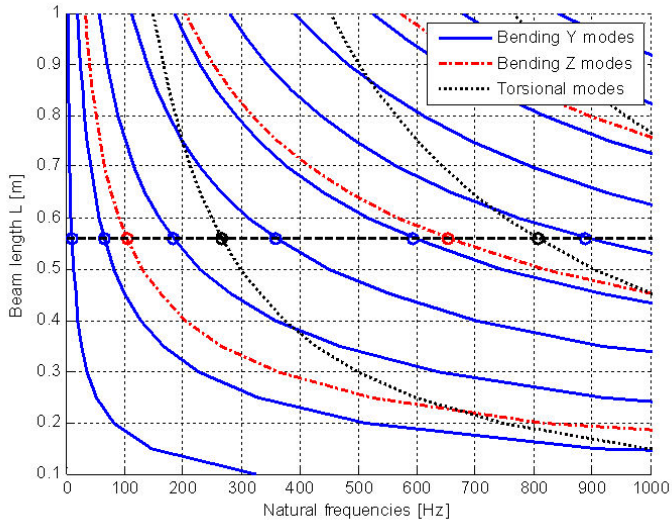

Figure 4.2: Effect of the length of the beam (section 40×4 mm) on the natural frequencies

The weight of the wings is designed using the same criteria so that the modes are well separated for most of the possible different configurations. The calculations provide an optimal mass of about 0.014 Kg. The effect of the added mass of the wings at the free end of the beam is shown in Figure 4.3.

The value of the natural frequencies of the first 10 modes obtained from a 3D finite element model are summarized in Table 4.1 for 3 different cases:

- Case 1 : Beam only without added mass of wings

- Case 2 : Beam with wings at 500 mm distance from clamp

- Case 3 : Beam with wings at 200 mm distance from clamp

The frequencies are reasonably separated and it is now possible to design the damping devices acting on the wings. Keeping the mass of the wings around 0.014 Kg means that the wings are quite small. This will affect the size of the magnets and the value of the normal load for Coulomb friction in order to obtain a useful value for damping coefficients.

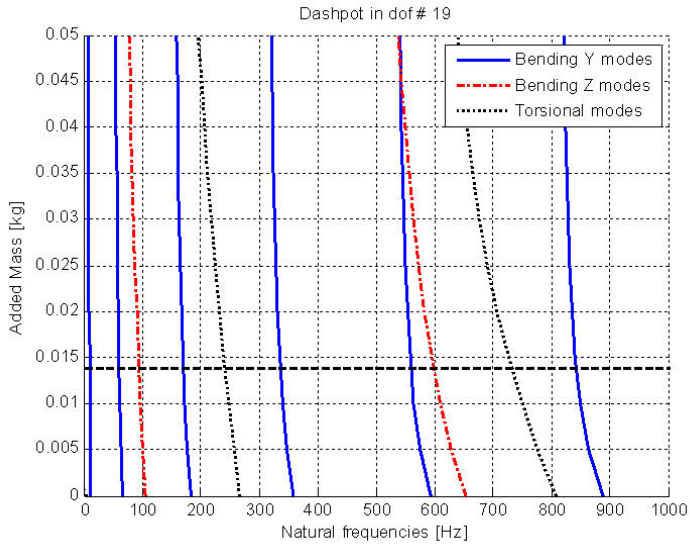

Figure 4.3: Effect of the added mass of wings on the natural frequencies

Mode	**Description**	**Freq.[Hz] case 1**	**Freq.[Hz] case 2**	**Freq.[Hz] case 3**
1	1^{st} bending xy	10.38	9.7256	10.536
2	2^{nd} bending xy	65.034	64.271	63.469
3	1^{st} bending xz	103.05	96.679	102.82
4	3^{rd} bending xy	181.98	182.42	177.66
5	1^{st} torsional	269.11	233.66	264.09
6	4^{th} bending xy	356.75	357.91	353.13
7	5^{th} bending xy	588.27	591.69	582.99
8	2^{nd} bending xz	628.73	623.06	606.53
9	2^{nd} torsional	809.35	754.52	684.69
10	6^{th} bending xy	885.38	885.09	873.69

Table 4.1: Natural frequencies of the beam in case 1, 2 and 3

4.4 Viscous dashpot design

In order to simulate the viscous damping, an eddy current dashpot has been designed. The movement of a conductor (the aluminium wing) through a stationary magnetic field (Figure 4.4) generates electromagnetic forces that creates a damping effect close to pure viscous damping [15]. By varying the air gap between the magnets is it possible to vary the damping coefficient of the dashpot very easily. This coefficient can be estimated if the size of the magnets and conductor are known [16]. Starting with the assumption that the total mass of wings must equal 0.014 Kg, the dimensions of the wings are 20×25×6 mm.

The useful section for the eddy current dashpot is 20×15×6 mm. To amplify the effect of the eddy currents, 2 rare-earth NdFeB magnets (one above and one below the wing) with residual magnetic induction 1.2 Tesla are used to create the magnetic field. The section parallel to the wing has been designed so that the damping effect is maximized, according to the calculation by Nagaya [16], without exceeding the size of the wing to avoid nonlinear edge effects of the

magnetic field (15×10 mm). The thickness of 30 mm provides a sufficient damping coefficient for the experiment, increasing this value doesn't change the damping coefficient considerably. To obtain bigger coefficients a new beam frequencies design with bigger wings should be required. Figure 4.5 shows the range of damping coefficient values available using these dimensions varying the air gap between magnets and wing.

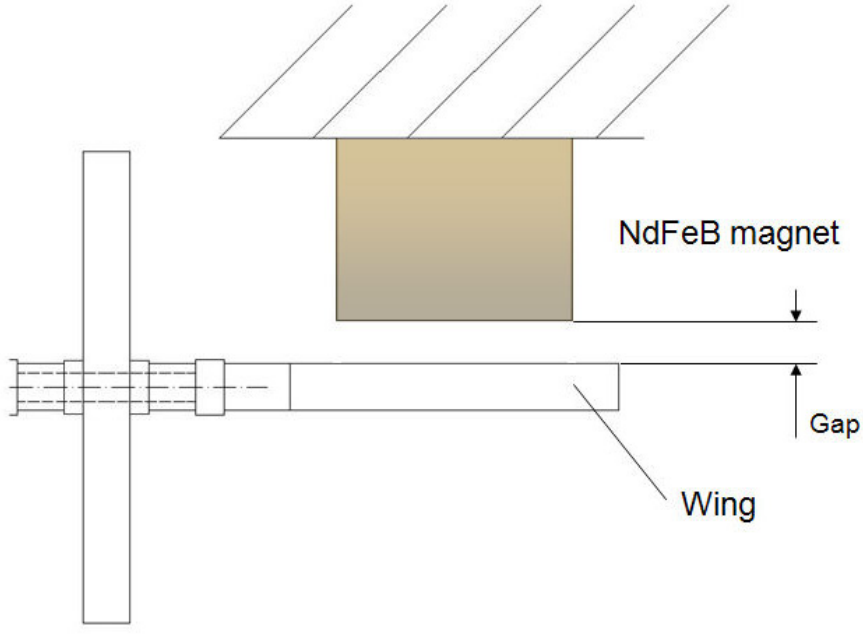

Figure 4.4: Sketch of the eddy current dashpot

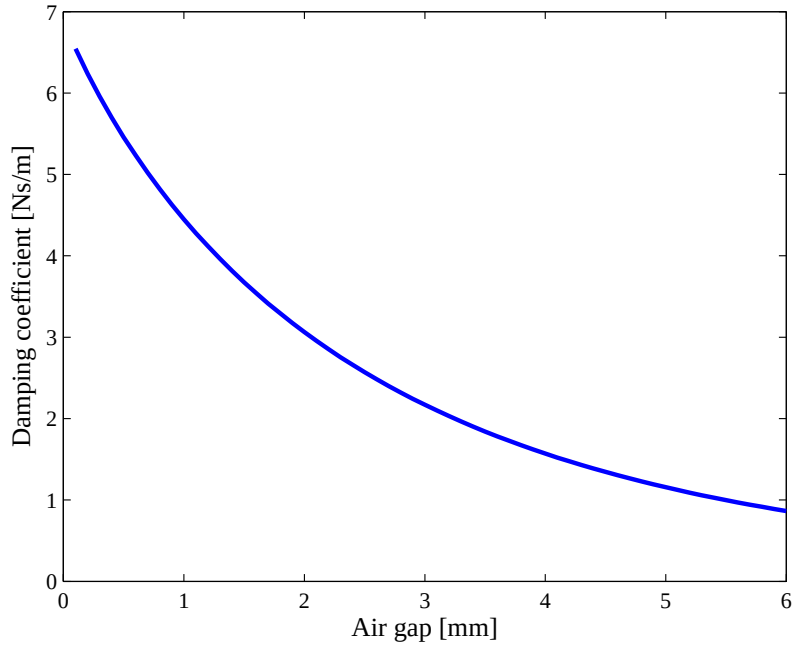

Figure 4.5: Damping coefficient versus air gap between magnets and wing

4.5 Coulomb friction dashpot design

The Coulomb friction dashpot simply consists of a calliper where different material films are attached acting on the wing as shown in Figure 4.6 (the thickness of the friction material in Figure 4.6 is exaggerated to become visible in the sketch). Material films can be applied to the wings too to provide different combination of materials. The normal force is provided by the screw in the middle of the calliper and it can be measured by static tests by a dynamometer applied in the contact point. The tangential force is measured by a force transducer located between the calliper and the support (the green square in Figure 4.6).

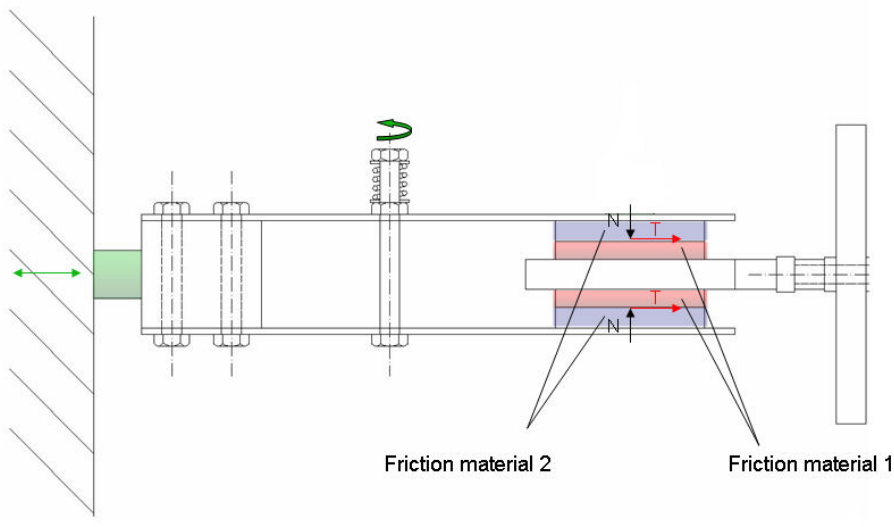

Figure 4.6: Sketch of the Coulomb friction device

Knowing the normal and tangential force is it possible to calculate the Coulomb friction coefficient to compare to the one obtained by damping identification.

4.6 Experiment photographs

The experimental setup (Figure 4.7) is almost ready, the only missing part is the eddy current magnetic dashpot. The magnets must be correctly characterised before being mounted on the structure so some preliminary tests are needed. Some initial tests were performed on the undamped structure and with Coulomb friction only.

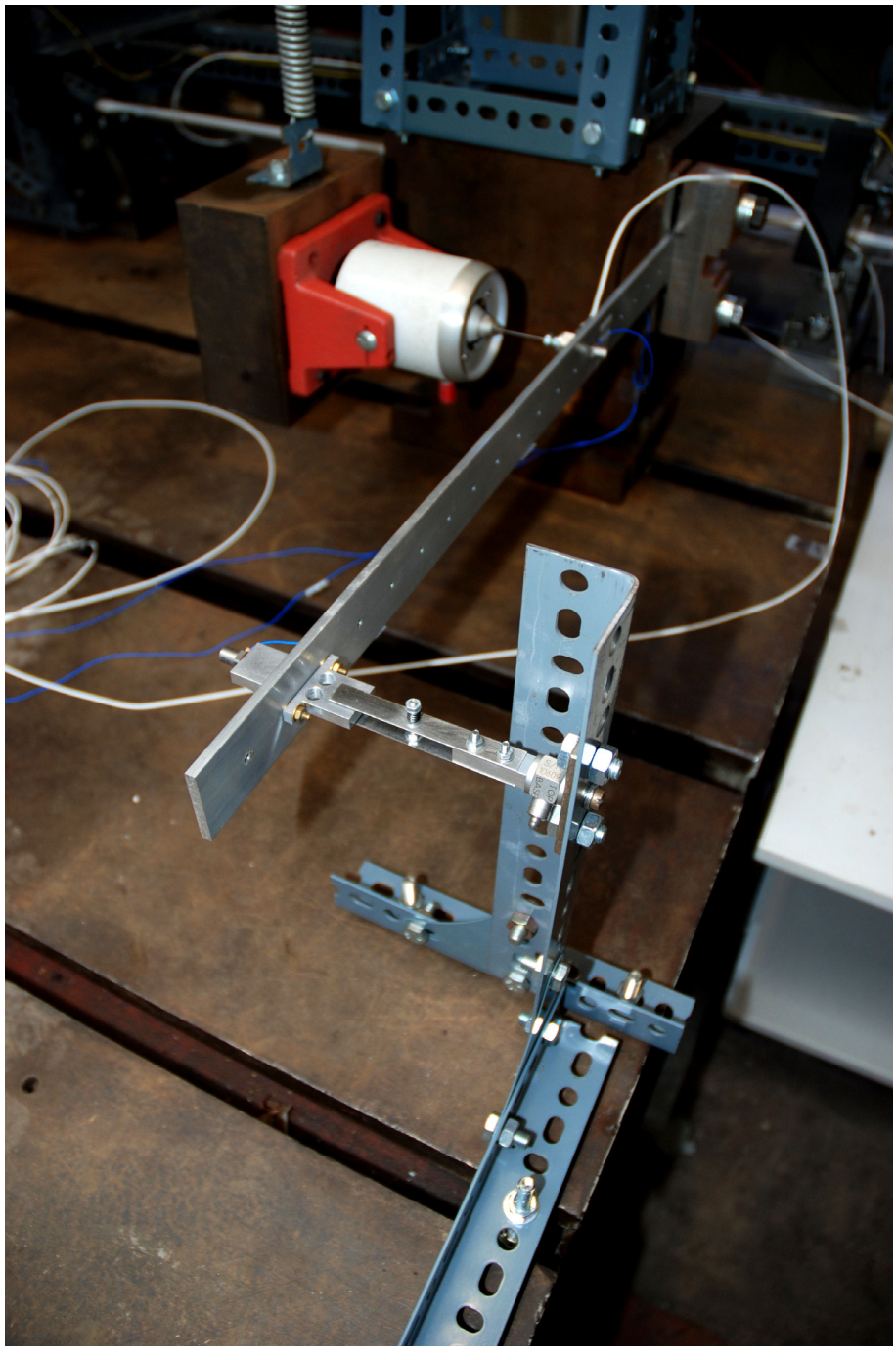

Figure 4.7: Experimental setup

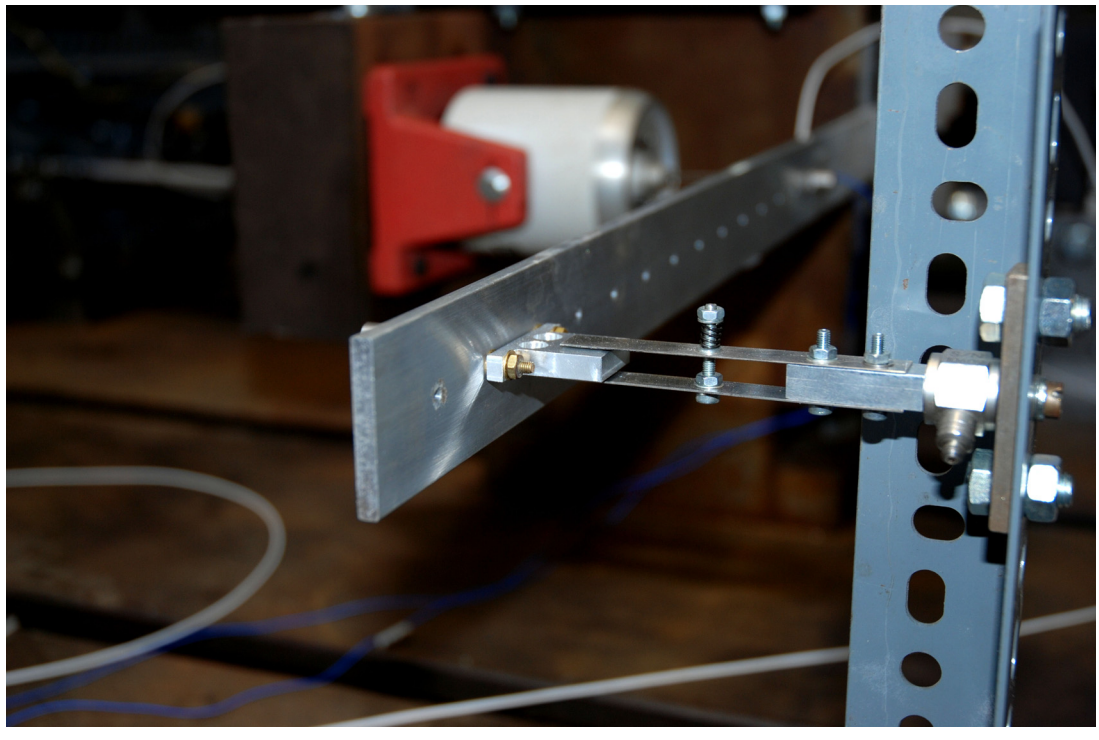

Figure 4.8: Coulomb friction device

Chapter 5

Conclusions

In this report a review of the existing damping identification techniques has been presented. From one of these techniques a new method has been developed to overcome some limitations of the original method. The method has been numerically validated with several different simulations. An experimental setup has been designed and built to test the method on a real case. Experiments started in June 2008.

Future works will include the validation of the method by the experiments and the extension of the method to include material damping (always present in real structures but still not implemented in the method). Alternative modelling of damping and different parametrizations of the matrices will be investigated. If the method is validated with successful results, an interesting application will be to test it on a Goland wing case, in order to obtain a better understanding of the effect of damping on aerostructure applications. Estimating the role of damping in aeroelastic instabilities will complete the research in the next year and a half.

Appendix A

In the next pages the technical drawings of the beam, the wings and dashpot devices are provided.

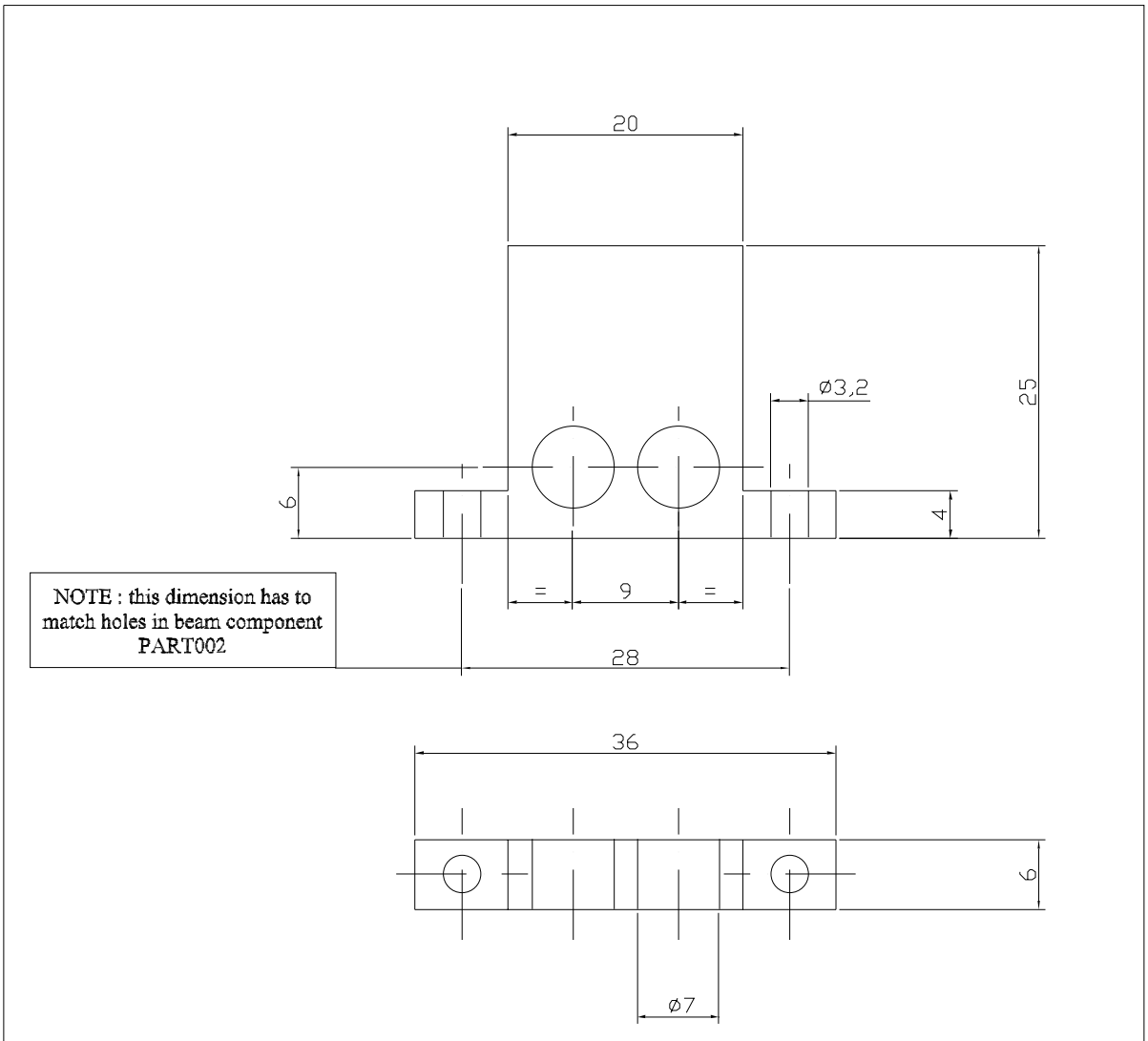

Issue A		Remarks	
		Approved by	
Original		Date	
		Drawn by	Marco Prandina
		Date	29-01-2008
		Scale	2 : 1
Part No. 001	Name of Part : Wing	Material : Aluminium	
Title: Wing		Drawing No.: PART001	
The University of Liverpool : Dept. of Engineering			

Figure 5.1: Wing

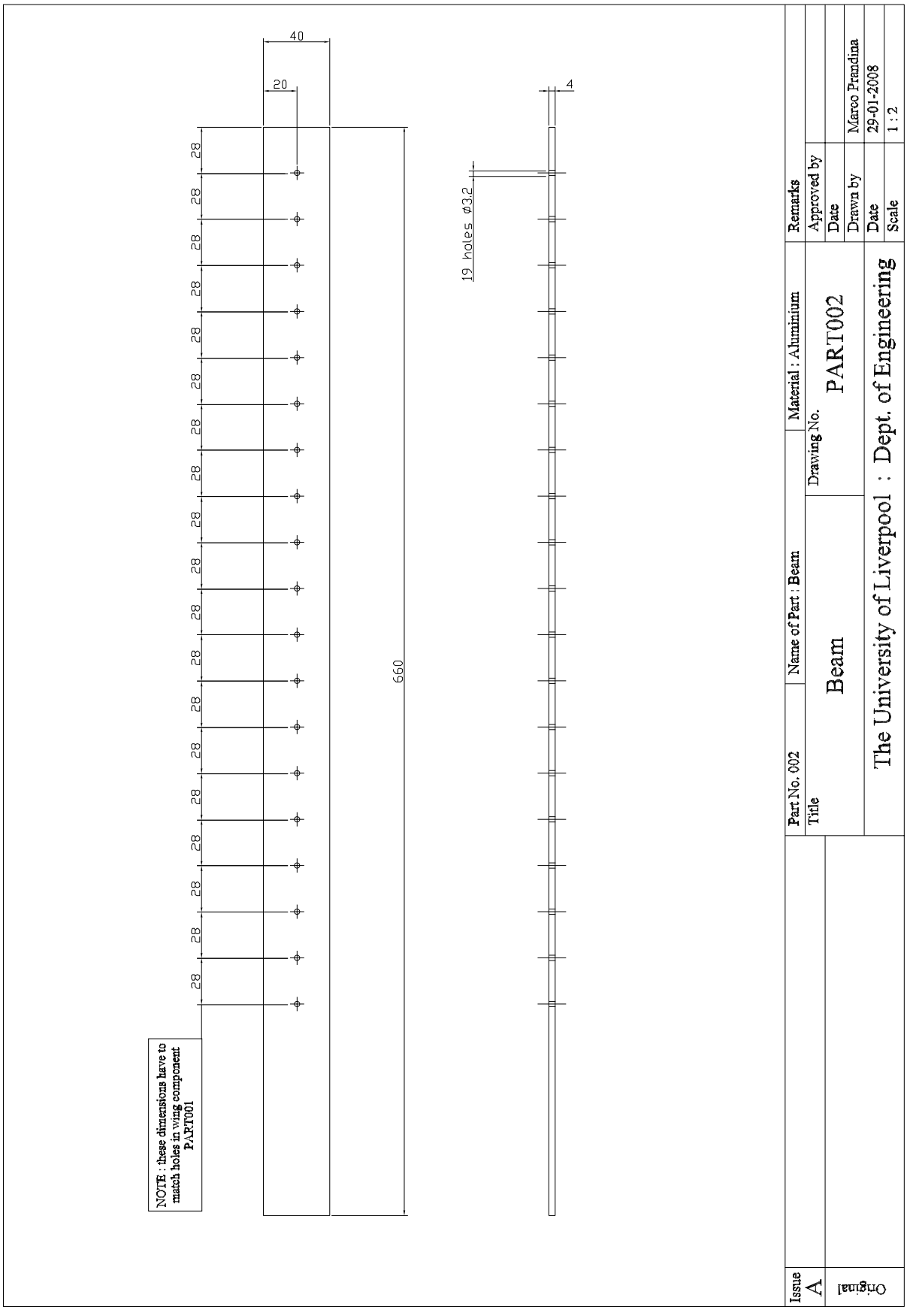

Figure 5.2: Beam

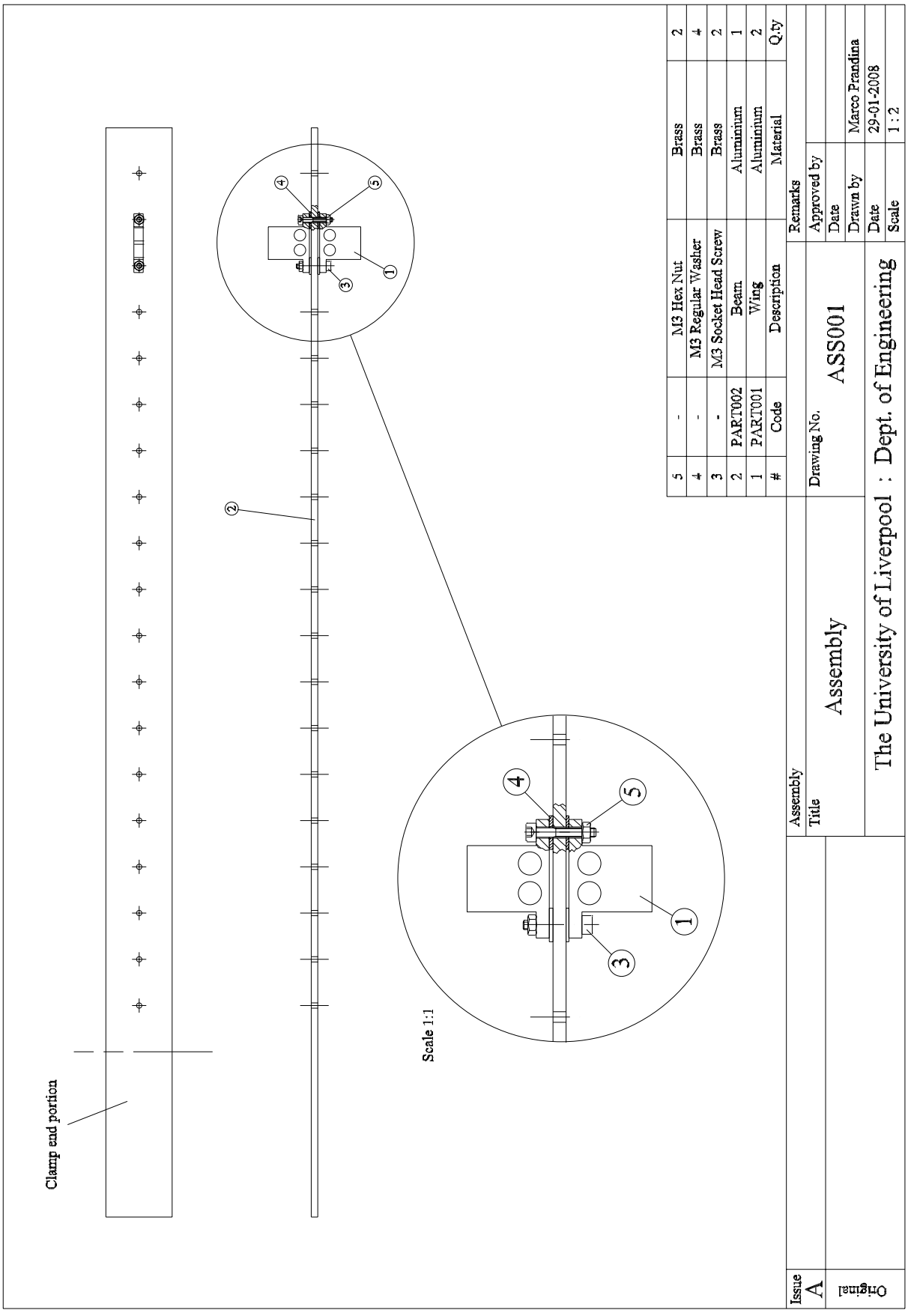

Figure 5.3: Wing and beam assembly

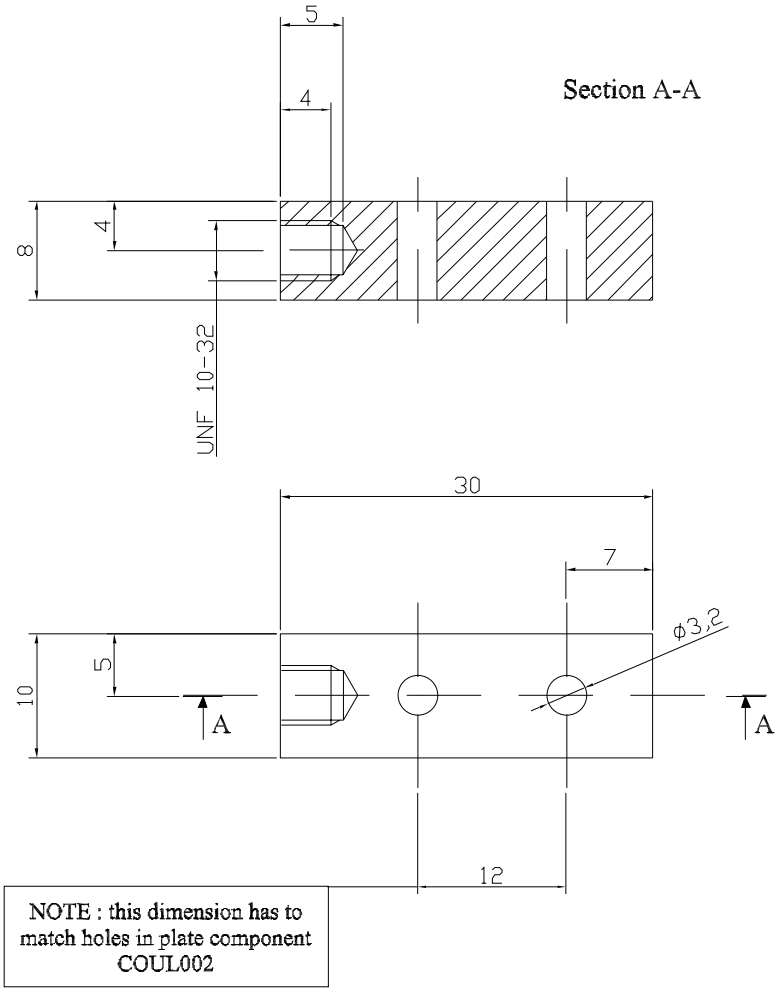

Issue A		Remarks	
		Approved by	
Original		Date	
		Drawn by	Marco Prandina
		Date	05-02-2008
		Scale	2 : 1
Part No. 003	Name of Part : Body	Material : Aluminium	
Title: Body		Drawing No.: COUL001	
The University of Liverpool : Dept. of Engineering			

Figure 5.4: Coulomb dashpot part 1

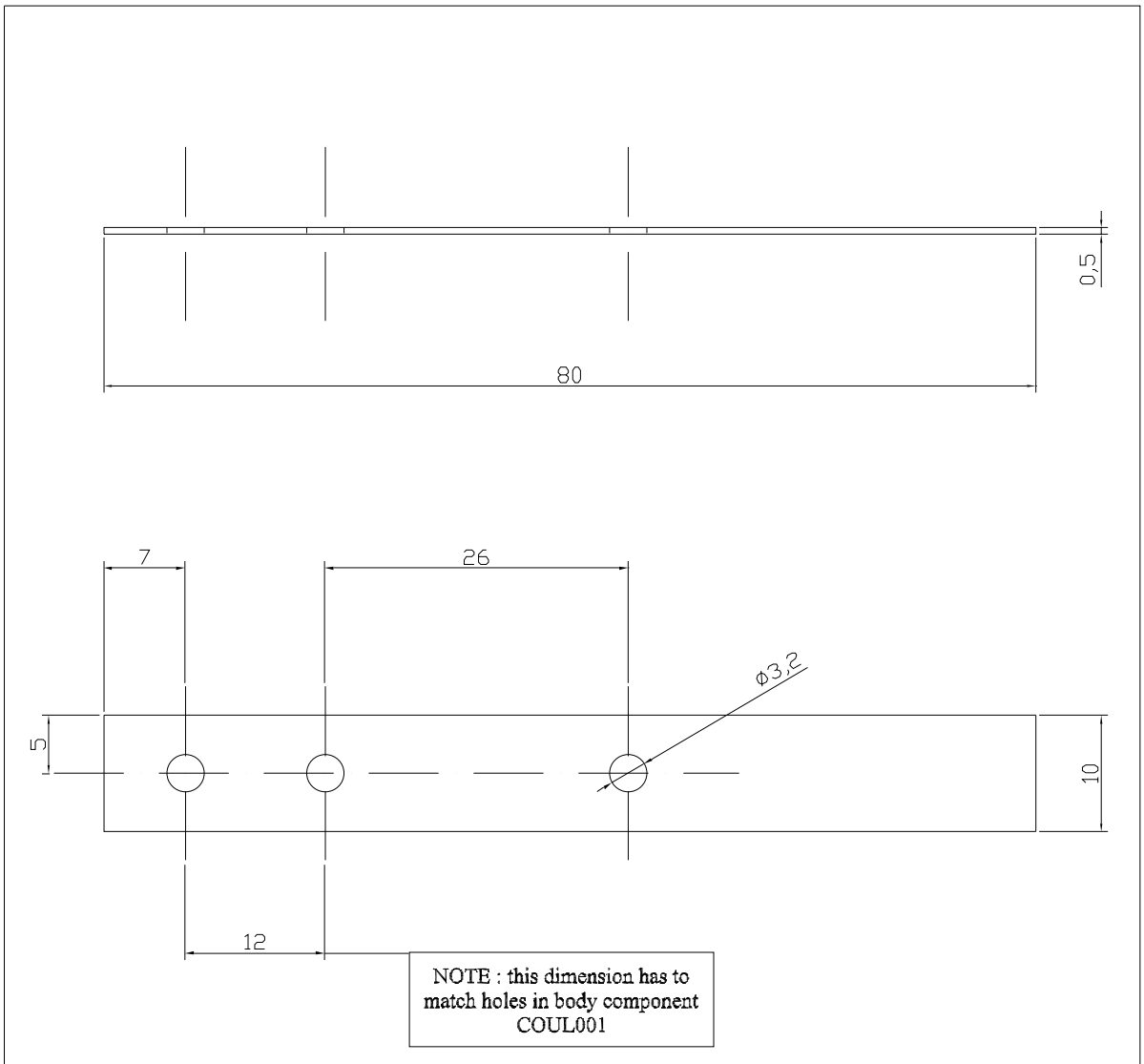

Issue A		Remarks	
		Approved by	
Original		Date	
		Drawn by	Marco Prandina
		Date	05-02-2008
		Scale	2 : 1
Part No. 004	Name of Part : Plate	Material : Aluminium	
Title: Plate		Drawing No.: COUL002	
The University of Liverpool : Dept. of Engineering			

Figure 5.5: Coulomb dashpot part 2

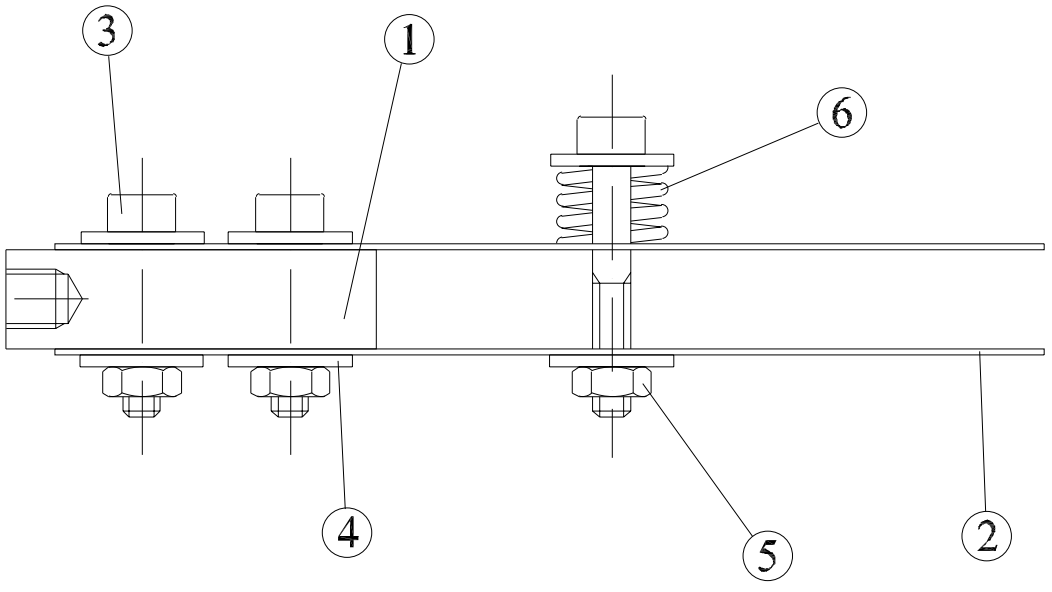

#	Code	Description	Material	Q.ty
6	-	Spring	Steel	1
5	-	M3 Hex Nut	Brass	3
4	-	M3 Regular Washer	Brass	6
3	-	M3 Socket Head Screw	Brass	3
2	COUL002	Plate	Aluminium	1
1	COUL001	Body	Aluminium	1

Issue A		Remarks	
		Approved by	
Original		Date	
		Drawn by	Marco Prandina
		Date	05-02-2008
		Scale	2 : 1

Assembly

Title	Drawing No.
Assembly 2	ASS002

The University of Liverpool : Dept. of Engineering

Figure 5.6: Coulomb dashpot assembly

Bibliography

[1] Adhikari S. and Woodhouse J. Identification of damping: part 1, viscous damping. *Journal of Sound and Vibration*, 243(1):43–61, 2001.

[2] Adhikari S. *Damping models for structural vibration*. PhD thesis, University of Cambridge, 2000.

[3] Lees A.W. Use of perturbation analysis for complex modes. In *Proceedings of the 17th International Modal Analysis Conference*, number 3727, pages 779–784, 1999.

[4] Pilkey F.D., Park G., and Inman D.J. Damping matrix identification and experimental verification. In *Proceedings of the SPIE's 6th Annual International Symposium on Smart Structures and Materials*, number 3672, pages 350–357, Newport Beach, California, 1999.

[5] Lancaster P. Expression of damping matrices in linear vibrations problems. *Journal of the Aerospace Science*, 28:256, 1961.

[6] Lancaster P. and Prells U. Inverse problems for damped vibrating systems. *Journal of Sound and Vibration*, 283:891–914, 2005.

[7] Link M. Using complex modes for model updating of structures with non proportional damping. In *Proceedings of the International Conference on Noise and Vibration Engineering (ISMA2006)*, pages 2593–2606, University of Leuven, Belgium, 2006.

[8] Lee J.-H. and Kim J. Development and validation of a new experimental method to identify damping matrices of a dynamic system. *Journal of Sound and Vibration*, 246(3):505–524, 2001.

[9] H. Lamarque C., Pernot S., and Cuer A. Damping identification in multi-degree-of-freedom systems via a wavelet-logarithmic decrement-part 1: theory. *Journal of Sound and Vibration*, 235(3):361–374, 2000.

[10] Liang J.-W. and Feeny B.F. Balancing energy to estimate damping parameters in forced oscillators. *Journal of Sound and Vibration*, 295:988–998, 2006.

[11] Liang J.-W. Damping estimation via energy-dissipation method. *Journal of Sound and Vibration*, 307:349–364, 2007.

[12] Jalali H., Ahmadian H., and Mottershead J.E. Identification of nonlinear bolted lap-joint parameters by force-state mapping. *International Journal of Solids and Structures*, 44:8087–8105, 2007.

[13] Friswell M.I., Mottershead J.E., and Ahmadian H. Combining subset selection and parameter constraints in model updating. *Transactions of the ASME*, 120:854–859, 1998.

[14] Bjorck A. and Golub G.H. Numerical methods for computing angles between linear subspaces. *Mathematics of Computation*, 27(123):579–594, 1973.

[15] Sodano H.A., Bae J.-S., Inman D.J., and Blvin W.K. Concept and model of eddy current damper for vibration suppression of a beam. *Journal of Sound and Vibration*, 288:1177–1196, 2005.

[16] Nagaya K. and Kojima H. Shape characteristics of a magnetic damper consisting of a rectangular magnetic flux and a rectangular conductor. *Bulletin of JSME*, 25(206):1306–1311, 1982.